Numerical Investigation of Lagrangian Single-Component Liquid Film Evaporation models

V. Ebrahimian[*a], C. Habchi[a] and B. Cuenot[b]
[a] IFP, 1 & 4, avenue de Bois Préau 92852 Rueil-Malmaison Cedex, France
[b] CERFACS, 42 avenue Gaspard Coriolis, 31057 Toulouse Cedex 01, France

Abstract

Liquid film evaporation from solid surfaces is of relevance to many engineering problems such as piston and turbine engines, exhaust system and even in spray cooling. In this study, a turbulent channel configuration with hot gas flow and liquid film on the lower wall has been investigated in order to study the effects of wall temperature, ambient gas temperature and turbulence on the evaporation of the liquid film. Two Lagrangian single-component liquid film evaporation models developed by O'Rourke and Amsden (OA) and by Desoutter et al. (GD), already implemented in the Reynolds Average Navier-Stokes (RANS) code IFP-C3D, have been applied to the channel configuration. The results of the study show that, in both Lagrangian liquid film models of OA and GD, the increase in the turbulence intensity, ambient gas and wall temperatures help to increase the liquid film evaporation. In addition, the comparison of the numerical results has shown a faster liquid film evaporation using the GD model.

Introduction

The necessity of liquid film evaporation model refers mainly to the system optimization in order to meet the environmental standards severization. For instance, the liquid film formed on the piston surface of engines, is one of the most important sources of unburned hydrocarbon (HC) and soot production especially during cold start [1,2]. In other systems such as Selective Catalytic Reduction unit (SCR), by injecting a reductant (such as urea-water solution) to the burnt gas, a liquid film may be formed on the wall that decreases the rate of NOx reduction. For this reason, a model that predicts the liquid film evaporation is needed.

In the past few decades, some experimental and numerical film evaporation studies have been performed [3-10]. Many multi-dimensional numerical models of liquid film have been developed by Stanton and Rutland [11, 12], Bai and Gosman [13], Foucart et al [14, 15], Han and Xu [16], O'Rourke and Amsden [17, 18] (referred to subsequently as OA) and Desouter et al [1] (referred to subsequently as GD). The first three models describe the dynamics of the liquid by an Eulerian approach whereas the models of GD and OA adopt a Lagrangian particle tracking method. Han & Xu improved the OA model by a new statistical treatment introduced for the momentum exchange between the impinging spray and the wall film. The first five models use some assumptions, such as simple diffusion of the species, which may lead to inaccurate results. Moreover, for the wall laws, the transition between the fully turbulent region and the viscous laminar sub-layer is assumed to occur at a constant value and is independent of the rate of evaporation.

The more recent model (GD) for liquid film evaporation uses new wall function [19] and better takes into account the blowing velocity due to evaporation, and the strong density and viscosity gradients near the liquid film.

Methods

Two Lagrangian single-component liquid film evaporation models developed by O'Rourke and Amsden [18], with some modifications in the model [20] and by Desoutter et al. [1], already implemented in the Reynolds Average Navier-Stokes (RANS) code IFP-C3D, are studied in this work.

In the OA model [18], the film thickness is calculated as the ratio of the volume of the parcels located on each cell face to the area of this cell face. This method has some disadvantages;

- a loss of film velocity since passing from a completely wetted wall face to the other completely dries
- an over-estimate of evaporation at the border of film
- mesh dependency of the model.

[*]Corresponding author, Email: vahid.ebrahimian@ifp.fr

These issues lead to propose a new method to calculate the mean film thickness [20]. This method estimates the surface wetted by each parcel on the wall [19]. This surface is used to calculate the film thickness at each parcel location. This method is also applied to the model of GD.

The main differences between the two models of OA and GD are the following:

- In the OA model, profile of temperature in the film is linear, while the GD model uses a third order polynomial film temperature profile.
- In the OA model, simple diffusion model is used, but the GD model takes into account the complex diffusion of the species in the gas boundary layer above the film.
- Based on direct numerical simulation (DNS) of liquid film evaporation in a turbulent channel, new mass, momentum and energy wall laws have been developed in the GD model in order to take into account the strong gradients of gas density and viscosity near the liquid film, and the gas boundary-layer blowing due to the film evaporation.

Case Study

To observe the effects of some parameters on the evaporation of liquid film and to compare their performances, both models of GD and OA are applied to the simple case of channel flow. The schematic of the calculation domain is shown in Figure 1.

In this study, a uniform mesh of $50\times15\times15$ cells is used. The mean flow is in the x direction. The initial gas pressure and temperature is *1 bar* and *300 K* respectively. A thin liquid film with the initial thickness h_f and temperature of *10* μm and *300 K* is located on the bottom wall of the channel. Within the Lagrangian approach, the liquid film is initialized by putting one parcel in each wall cell-face as shown in Figure 2. The volume of each parcel is therefore,

$$V_f = h_f . A_f \qquad (1)$$

where A_f is the area of each wall cell-face. To avoid the liquid film to go out the channel wall, the film velocity is assumed to be zero. Thus, the liquid film is maintained in the computational domain. The gas consists of *nitrogen* and the liquid is *n-heptane*. The inlet mass flow rate and temperature and the outlet static pressure conditions are specified and the calculation is done for different cases reported in Table 1.

Results and Discussion

The effect of Wall Temperature, Gas Temperature and Turbulence on the film evaporation is investigated. The results are shown in Figure 3 to Figure 5. The mean parameters plotted in these Figures are obtained at each time step by a weighted average using the local parcel surface. In all figures, the film thickness decreases with time due to evaporation. The film evaporation phenomenon consists of two periods. The transient period in which the heat transferred to the film is dedicated to both augment the film temperature and evaporate it. In this period which lasts *10 ms* approximately, most of the heat is consummated to increase the film temperature. And the steady period when the heat transfer to the film mostly evaporates the liquid film. These two periods can be distinguished in Figure 3 to Figure 5.

Effect of Wall Temperature on the Evaporation of Liquid Film

Figure 3 shows the effect of wall temperature on the mean film surface temperature (Figure 3(a)), mean film thickness (Figure 3(b)) and mean evaporation rate (Figure 3(c)). In this case, the gas temperature and Reynolds number have the constant values of *300 K* and *10000* respectively. It could be observed that there is a short transient period where the film surface temperature increases (Figure 3(a)) (at the first part of the curve) that causes an increase in the evaporation rate of the film (Figure 3(c)). After a small time, the film surface temperature reaches a value close to the specified wall temperature. One can also see that the film thickness (Figure 3 (b)) decreases with increasing the wall temperature.

Effect of Turbulence on the Evaporation of Liquid Film

To observe the effects of turbulence in the evaporation of liquid film, three different Reynolds numbers are applied to the channel flow with constant wall and gas temperatures of *330 K* and *300 K* respectively. The result of

Turbulent Kinetic Energy (TKE) for these cases is also shown in Figure 4(d). The TKE curve is drawn as a function of horizontal distance from the beginning of liquid film (Black arrow close to the liquid film and in the gas phase which is shown in Figure 1). In this Figure, by increasing the Reynolds number, the TKE increases. The rate of evaporation increases with the turbulence level (Figure 4(c)). Contrary, film thickness (Figure 4(b)) and film surface temperature (Figure 4(a)) decrease with increasing the turbulence level.

Effect of Gas Temperature on the Evaporation of Liquid Film

To observe the effect of gas temperature on the evaporation, the wall temperature is held constant at $330K$ and the results are obtained for the Reynolds number at 10000 .
As can be seen from Figure 5(a) to (c), increasing the gas temperature, results in an increase of the film surface temperature and evaporation rate of film. Consequently, the film thickness decreases.

Comparison of the OA and GD models

The two models of OA and GD are compared in Figure 3 to Figure 5. One can observe that for the mean film surface temperature case, and at the beginning of the evaporation, the surface temperature of GD model is less than OA model. This is because of the higher evaporation rate of the GD model than the OA model particularly during the transient period (Figure 3(c), Figure 4(c) and Figure 5(c)). It should be remarked that at the higher Reynolds numbers and at the higher gas and wall temperatures, because of the oscillating behavior of the gas pressure in the channel, the GD model has some oscillation in the evaporation rate. At the beginning of Figure 3(a), Figure 4(a) and Figure 5(a), film evaporation of the GD model leads to a cooling film phenomenon that decreases the film surface temperature of GD model compared to the OA model. This behavior is more visible in Figure 3(a). But, finally the surface temperature of the film reaches the same value for the two models. From Figure 3(b), Figure 4(b) and Figure 5(b), one can also see that the liquid film thickness reduces more in the GD model than OA model. Moreover, one can observe an increase of the film thickness at the beginning of the evaporation process using OA model. In fact, IFP-C3D code allows the density of liquid to vary as a function of temperature. At the beginning of the calculation and during the transient period, the heat transferred to the film increases the temperature of the film that leads to a decrease in the liquid film density and an increase in the liquid film volume; therefore, the film thickness of the film increases. In the steady period, contrary to the transient period, the transferred heat to the film is used mainly to evaporate the liquid film that decreases the liquid film thickness. In the GD model, because of the fast evaporation of the film, this phenomenon could not be observed. The basic features of the GD model and the present numerical results seem to indicate a better global behavior of the GD model.

Conclusions

In this paper, the effects of wall temperature, gas temperature and turbulence on the film evaporation are investigated. Two film evaporation models of OA and GD were compared in a turbulent channel test case and from the numerical results the following comments and conclusions are made:

- The gas temperature is a parameter that affects the film evaporation rate. By increasing the gas temperature at the constant wall temperature, the evaporation rate of the film increases.
- By increasing the turbulence in the channel, the film evaporation rate increases.
- Wall temperature has a significant effect on the evaporation of liquid film; the higher the wall temperature, the faster evaporation of liquid film. It seems that the effect of wall temperature on evaporation of film is more significant than the effect of the two other parameters. In this study, the wall temperatures are less than the saturation temperature of the n-heptane in order to avoid the effects of film boiling.
- It is shown that the rate of evaporation of the GD model is higher than that of the OA model. Comparison of the numerical results of OA and GD models with experiments is necessary to assess their validity.

References

1. Desoutter, G., Habchi, C., Cuenot, B., Poinsot, T., *International Conference on Atomization and Spray Systems*, Kyoto, Japan, 2006.
2. Habchi, C., Foucart, H., and Baritaud, T., Oil & Gas Science and Technology-Rev. IFP, Edition Technip, 54:211-222 (1999).
3. McBain, G.D., Suehrcke, H., Harris, J.A., Int. J. Heat Mass Transfer 43:2117-2128 (2000).

4. Beverley, K.J., Clint, J.H., Fletcher, P.D.I., Phys. Chem. Chem. Phys. 2:4173–4177 (2000).
5. Kelly-Zion, P.L., Pursell, C.J., Booth, R.S., VanTilburg, A.N., Int. J. Heat Mass Transfer 52:3305–3313 (2009).
6. Pauken, M.T., Exp. Therm. Fluid Sci. 18:334-340 (1999).
7. Himmelsbach, J., Noll, B., Wittig, S., Int. J. Heat Mass Transfer 37:1217–1226 (1994).
8. Gerendas, M., Wittig, W., J. Eng. Gas Turb. Power 123:580–588 (2001).
9. Brighton, P.W.M., J. Hazard. Mater. 23:215-234 (1990).
10. Chebbi, R., Hamam, S.E.M., Al-Kubaisi, M.K.M., Al-Jaja, K.M., Al-Shamaa, S.A.M., J. Chem. Eng. Jpn. 36:1510-1515 (2003).
11. Stanton, D.W., Rutland, C.J., *SAE Paper* 960628 (1996).
12. Stanton, D.W., Lippert, A.M., Reitz, R.D., Rutland, C.J., *SAE Paper* 982584 (1998).
13. Bai, C., Gosman, A.D., *SAE Paper* 960626 (1996).
14. Foucart, H., *PhD Thesis, Université de Rouen*, 1998.
15. Foucart, H., Habchi, C., LeCoz, J.F., Baritaud, T., *SAE Paper* 980133 (1998).
16. Han, Z., and XU, Z., *SAE Paper* 2004-01-0099 (2004).
17. O'Rourke, P., and Amsden, A., *SAE Paper* 96961 (1996).
18. O'Rourke, P., and Amsden, A., *SAE Paper* 2000-01-0271 (2000).
19. Desoutter, G., *PhD Thesis, Institut National Polytechnique de Toulouse*, 2007.
20. Habchi, C., "Modélisation de l'interaction spray/paroi dans les moteurs à combustion interne," IFP Report No. 59166, 2006.

Table 1. Case studies in this work

	Wall Temperature (K)	Reynolds Number	Gas Temperature (K)	Inlet Mass Flow Rate (kg/s)
Wall Temperature	310 330 350	10000	300	54e-4
Reynolds Number	330	5000 10000 15000	300	27e-4 54e-4 81e-4
Gas Temperature	330	10000	300 450 600	54e-4

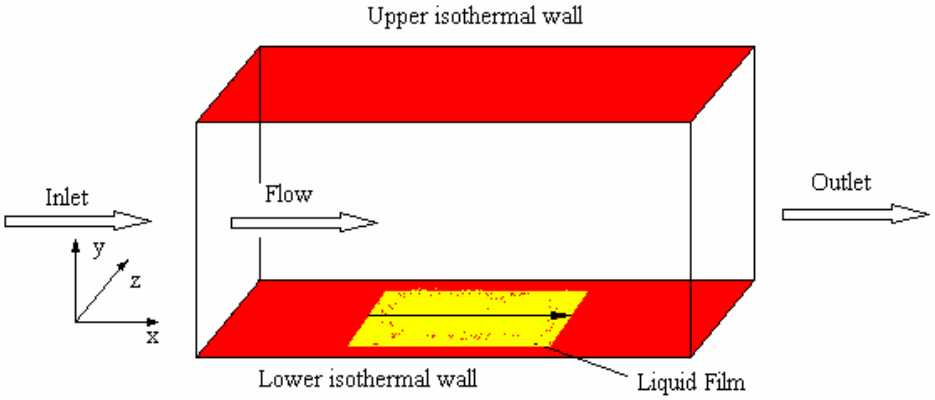

Figure 1. Schematic of the domain of the Channel-Test.

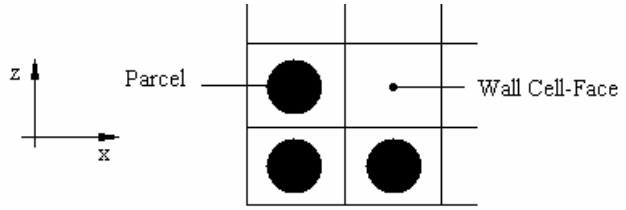

Figure 2. Schematic of Initialization of the film on the wall of Channel.

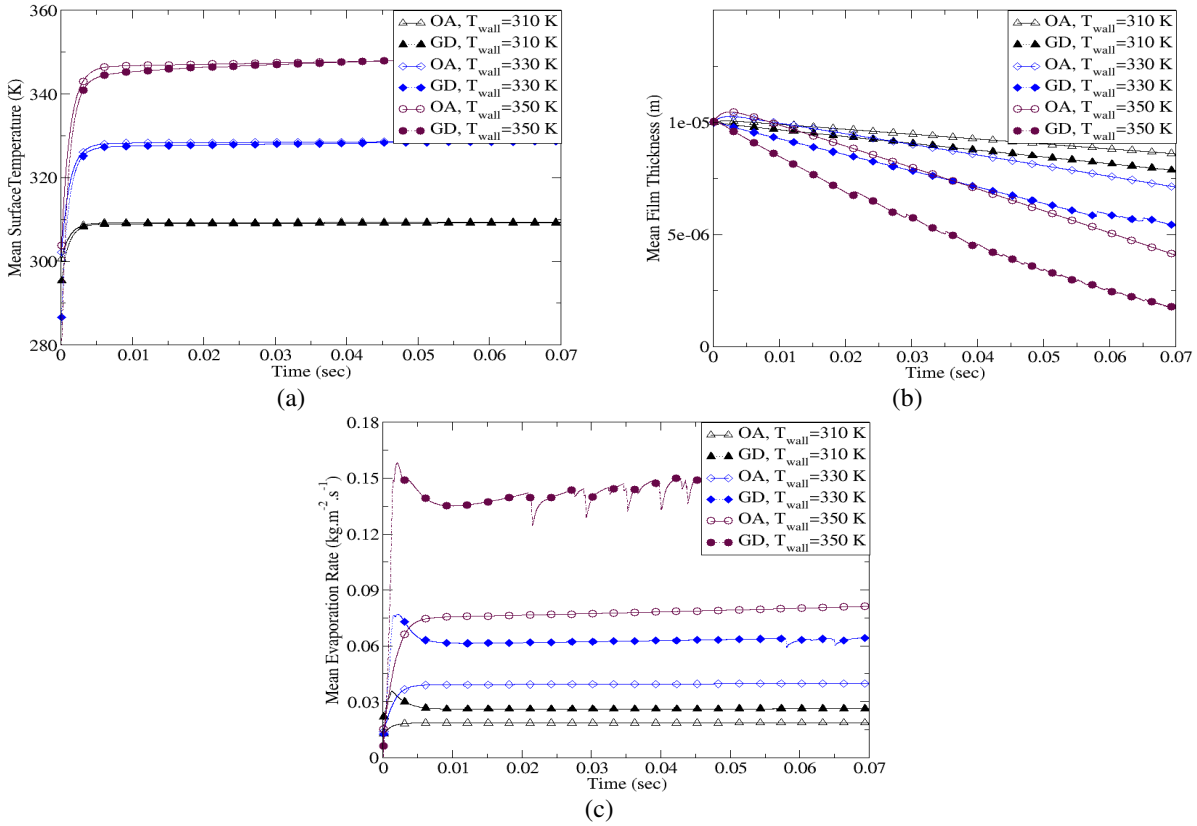

Figure 3. Behavior of liquid film for the OA and GD models and different wall temperatures at Tgas=300 K, Re=10000.

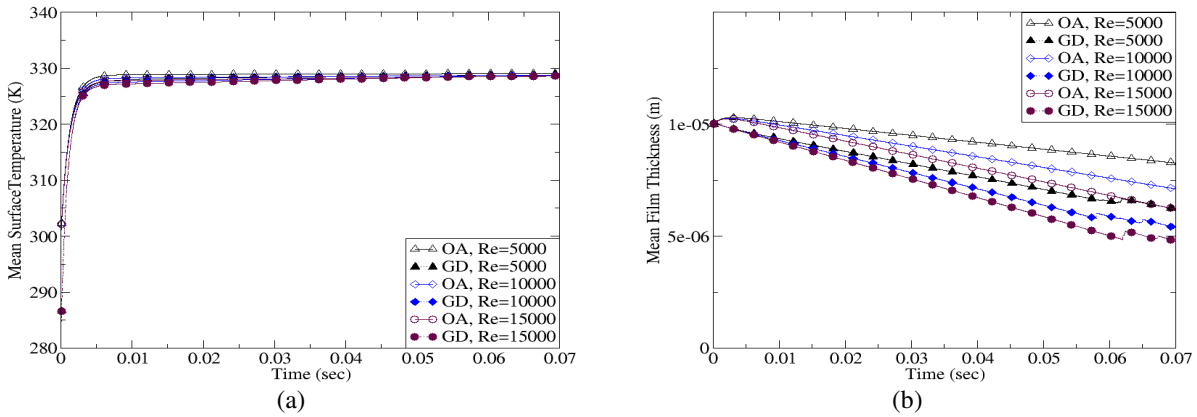

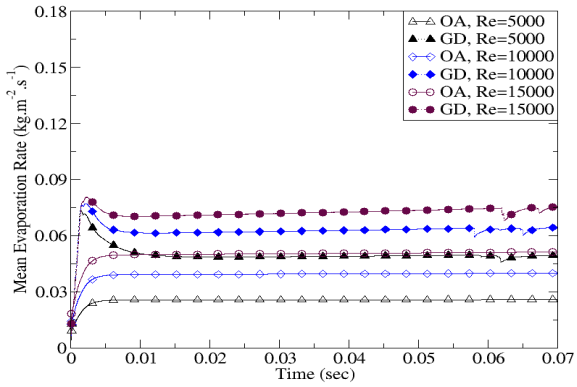

(c)

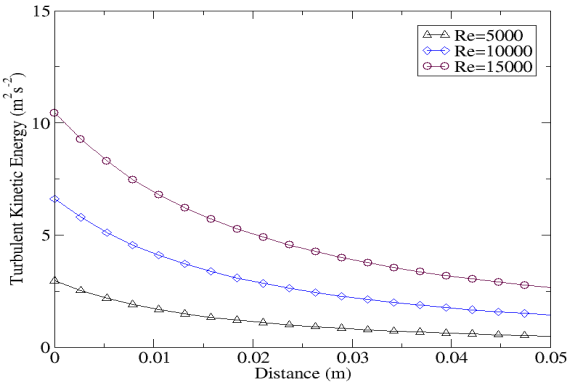

(d)

Figure 4. Behavior of liquid film for the OA and GD models and different Reynolds number at Tgas=300K, Twall=330 K.

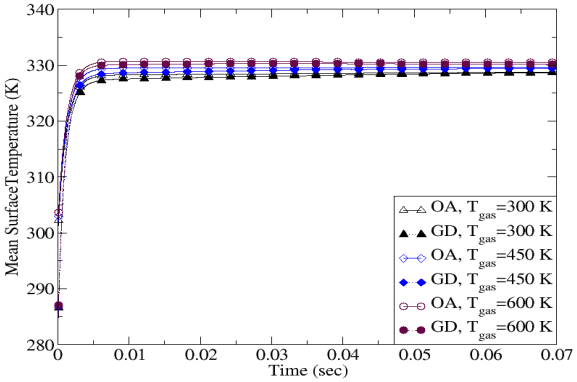

(a)

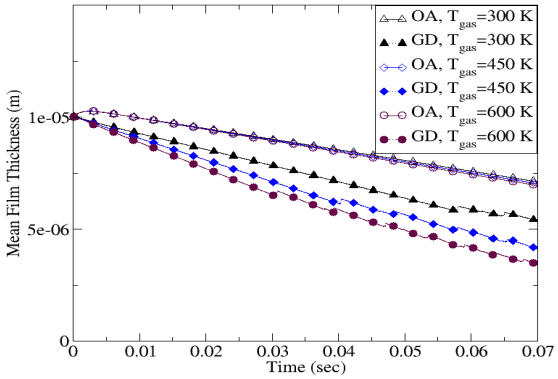

(b)

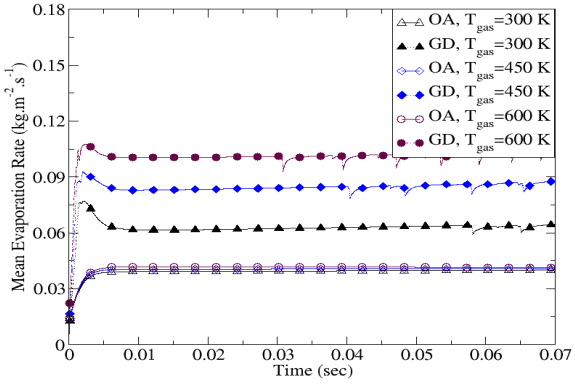

(c)

Figure 5. Behavior of liquid film for the OA and GD models for the different gas temperatures at Twall=330K, Re=10000.